Contribution of Dislocations to the Zero-Bias Resistance-Area Product of LWIR HgCdTe Photodiodes at Low Temperatures

Vishnu Gopal and Sudha Gupta

***Abstract*—Dislocations in the base material are shown to significantly influence zero-bias impedance of long wavelength infrared HgCdTe photodiodes by acting as a shunt, and by influencing their minority carrier lifetime. Consequently, temperature dependence of zero-bias resistance-area product (R_0A) of these photodiodes can be described very well over a broad temperature range, down to 25 K, after taking into account the temperature and dislocation dependence of the minority carrier lifetime in addition to the shunt resistance contribution of dislocations. Further, based on the theoretical prediction that the shunt resistance contribution of a dislocation is a sensitive function of the magnitude of the charge around its core, it is proposed that the scatter of the R_0A experimental data in diodes with dislocation densities of less than 1×10^7 cm^{-2} could be the result of statistical variations in the charge around the core of dislocations. Interaction of dislocations among themselves may be responsible for deviations above dislocation densities of 1×10^7 cm^{-2}.**

***Index Terms*—Dislocations, HgCdTe photodiodes, R_0A product.**

I. Introduction

IN A PREVIOUS paper [1], the effect of dislocations on the zero-bias resistance-area product, quantum efficiency, and spectral response of long wavelength infrared (LWIR) HgCdTe photodiodes was modeled by assuming the dislocations as the discontinuity in the lattice. The model provided an excellent fit to the experimental data of Johnson *et al.* [2] at dislocation densities of less than 10^7 cm^{-2} up to a temperature of 50 K. Below 50 K, the observed deviations between the model and the experimental data were qualitatively assigned to the tunneling currents, whereas the deviations above dislocation density of 10^7 cm^{-2} were assigned to the clustering of dislocations. It will now be shown that dislocations, besides operating as a shunt, also influence the diode impedance through their effect on minority carrier lifetime. It has been, thus, found that the model fits the experimental data well over the entire temperature range if, in addition to the dislocation dependence, the temperature dependence of minority carrier lifetime is also included in the model. The role of interacting dislocations in the high dislocation density range will also be discussed.

Manuscript received January 19, 2004; revised April 13, 2004. The review of this paper was arranged by Editor L. Lunardi.

The authors are with the Solid State Physics Laboratory, Timarpur, Delhi 110054, India (e-mail: vishnu_gopal/sspl@ssplnet.org).

Digital Object Identifier 10.1109/TED.2004.829857

II. Model

In this section, the presentation of the model has been divided into two parts. Part A of the model deals with the calculation of the temperature and dislocation dependence of minority carrier lifetime in HgCdTe material. Part B is essentially the summary of the model reported previously [1] and describes the calculation of zero-bias impedance of a p^+-n Hg_{1-x} Cd_xTe diode.

A. Dislocation and Temperature Dependence of Minority Carrier Lifetime

Dislocations in a material are the regions of high recombination and have been shown [1] to influence the diffusion length of the minority carriers according to the following interrelation between dislocation density (N cm^{-2}) and the diffusion length L_h

$$\frac{1}{L_h^2} = \frac{1}{L_0^2} + \frac{2\pi \text{mas} N}{D_h} \tag{1}$$

where L_0 is the diffusion length of minority carrier in the absence of dislocations, D_h is their diffusion coefficient, m is an integer with minimum value of unity, which means that the radius of dislocation cylinder is equal to one lattice constant a, and s is the carrier recombination velocity at the dislocation site.

Relation (1) can be rewritten in terms of minority carrier lifetime as follows:

$$\frac{1}{\tau_h} = \frac{1}{\tau_0} + 2\pi \text{mas} N. \tag{2}$$

In the above equation, the second term on the right hand side represents the contribution of dislocations and the contributions from all other known mechanisms, namely, Radiative, Auger, and Shockley–Read (SR) recombination are included in τ_0. Equation (2) can be thus used to calculate the temperature and dislocation dependence of minority carrier lifetime in a given material using the well-known theoretical expressions for the various recombination mechanisms. For the sake of completeness, the relevant expressions required to calculate the minority carrier lifetime in an n-type HgCdTe material are summarized in the following paragraphs.

1) Radiative Recombination: The radiative process involves direct band-to-band recombination of a conduction-band electron with a heavy hole and the emission of a photon. The radiative lifetime is given by [3], [4]

$$\tau_R = \frac{n_i^2}{B(n_0 + p_0)} \tag{3}$$

where n_i is the intrinsic electron concentration, n_0 and p_0 are the thermal equilibrium concentrations for electrons and holes, respectively, and B is the thermal equilibrium spontaneous generation rate given by [3], [4]

$$B = 5.8 \times 10^{-13} n_i^2 \varepsilon_\infty^{1/2} \left(\frac{m_0}{m_e^* + m_v^*}\right)^{3/2} \left(1 + \frac{m_0}{m_e^*}\frac{m_0}{m_v^*}\right) \times \left(\frac{300}{T}\right)^{3/2} \left[E_g^2 + 3kTE_g + 3.75(kT)^2\right] \quad (4)$$

where ε_∞ is the high-frequency dielectric constant, E_g is the energy bandgap, k is Boltzmann's constant, T is the temperature, and m_e^*, m_v^*, and m_0 are the effective electron, effective hole, and the electron rest mass, respectively.

2) Auger Recombination: The Auger-1 process is believed to be the dominant recombination mechanism in n-type HgCdTe [4]. This process involves the direct band-to-band recombination of a conduction band electron with a heavy hole and the excitation of another electron in the conduction band. The intrinsic lifetime for the Auger-1 process is [4]–[6]

$$\tau_{A1}^{(i)} = 3.8 \times 10^{-18} \varepsilon_\infty^2 \frac{m_0}{m_e^*}(1+\mu)^{1/2}(1+2\mu) \times \left(\frac{E_g}{kT}\right)^{3/2} \exp\left(\frac{1+2\mu}{1+\mu}\frac{E_g}{kT}\right) |F_1F_2|^{-2} \quad (5)$$

where μ is the ratio of electron to hole effective masses, ε_∞ is the high frequency dielectric constant, E_g is the energy gap, and $|F_1F_2|$ is the overlap integral of the Bloch functions, whose value ranges between 0.1 to 0.3 [3]. It has always been treated as an adjustable parameter to fit the experimental data.

The extrinsic lifetime for the Auger-1 process can be expressed as [4]–[6]

$$\tau_{A1} = \frac{2n_i^2}{(n_0+p_0)n_0}\tau_{A1}^{(i)} \quad (6)$$

3) SR Recombination: The steady-state lifetime of excess holes due to SR recombination via a level at $E_{\rm ts}$ above the valence-band edge can be expressed as [4], [7]

$$\tau_p = \frac{\tau_{p0}(n_0+n_1) + \tau_{n0}(p_0+p_1) + \tau_{p0}N_{\rm ts}(1+p_1/p_0)^{-1}}{n_0 + p_0 + N_{\rm ts}(1+p_0/p_1)^{-1}(1+p_1/p_0)^{-1}} \quad (7)$$

where $\tau_{p0} = 1/(\sigma_p v_{\rm th} N_{\rm ts})$, and $\tau_{n0} = 1/(\sigma_n v_{\rm th} N_{\rm ts})$. $v_{\rm th}$ and $\sigma_{p,n}$ are the thermal velocity and capture cross sections for holes and electrons, and $N_{\rm ts}$ is the SR center concentration. Also $n_1 = n_i \exp[-(E_{\rm ts} - E_i)/{\rm kT}]$, and $p_1 = n_i \exp[-(E_i - E_{\rm ts})/{\rm kT}]$, where E_i is the intrinsic fermi energy level, and $E_{\rm ts}$ is the corresponding energy level of the SR centers.

In our recent study on the effect of dislocations on minority carrier lifetime, it has been reported [8] that dislocations contribute to the carrier recombination in more than one way. One way for carriers to recombine is through the modification of the energy band diagram due to the discontinuity of the lattice created by the dislocations, and the second way of recombination is through the SR type process on account of the generation of point defects by dislocations. The latter can be taken care of by calculating τ_{n0} and τ_{p0} from the following relation:

$$\tau_{n0}, \tau_{p0} = \frac{0.76}{N} + 4 \times 10^{-8}. \quad (8)$$

The above expression is the equation of the straight line shown in [8, Fig. 4] and applies to n-type HgCdTe material.

4) Recombination Contribution due to Dislocations: It can be seen from (2) that the calculation of dislocation contribution to the minority carrier life time requires a knowledge of the dislocation recombination velocity s. The latter can be estimated [1], [9] by using the following expression:

$$s = \frac{\sqrt{K_nK_p}N_t(n_0+p_0)}{2n_i\{\cosh[(E_T-E_i)/kT - u_0] + \cosh(qU_S/kT - u_0)\}} \quad (9)$$

where K_n and K_p, are, respectively, capture probabilities for electrons and holes by the surface states at the core of the cylindrical dislocation, q is the fundamental charge on an electron, N_t is the density of surface states at each dislocation, and E_t is the corresponding energy level of these states. Although the discontinuity of the lattice at dislocations may give rise to a series of levels within the bandgap of the material, however, those energy levels which significantly contribute to the recombination current are assumed to be distributed in a narrow range of energy and for the sake of simplicity may be approximated to a single level located at an energy level E_t. E_i is the intrinsic Fermi level in the bulk, and u_0 is defined as [9]

$$u_0 = \ln\sqrt{K_p/K_n}. \quad (10)$$

The potential U_s at the surface of the core of the dislocation can be determined by the combination of following equations [9]:

$$Q_{\rm SC} = q(n_0+p_0)L_{\rm db}F_t \quad (11)$$

$$F_t = \sqrt{2}\left\{\frac{\cosh(u_b+v_s)}{\cosh u_b} - v_s\tanh u_b - 1 + \frac{N_t^*}{n_0+p_0} \times \left[\ln\left(1+\frac{\exp(v_s)-1}{1+\exp(E_T/kT)}\right) - \frac{v_s}{1+\exp(E_T/kT)}\right]\right\}^{1/2} \quad (12)$$

where N_t^* is the trap density in the space charge region. In the absence of any knowledge about the value of N_t^*, it is assumed that the strain field generated at the discontinuity causes approximately the same number of trap levels within the space charge region. The value of N_t^* has been thus taken to be numerically equal to the value of density of surface states, that is, $N_t^* = 10^{15}$ cm^{-3}. u_s and v_s are the reduced potentials defined by the equations

$$u_s = qU_s/kT$$
$$v_s = q(U_s - U_b)/kT \quad (13)$$

where U_b is the potential in the bulk of the material, and the effective Debye length $L_{\rm db}$ is given by

$$L_{\rm db} = \sqrt{\frac{\varepsilon\varepsilon_s kT}{q^2(n_0+p_0)}} \quad (14)$$

where ε is the permittivity of the free space, and ε_s is the static dielectric constant of the mercury cadmium telluride material.

It has been already shown [8] that the above approach to model the lifetime can describe the dislocation and temperature dependence of the minority carrier lifetime very well over a broad range of temperature and dislocation densities, in a variety of HgCdTe samples including bulk samples, molecular beam

epitaxy, and metal–oxide chemical vapor deposition-grown epilayers on CdZnTe and GaAs substrates.

B. Calculation of Zero-Bias Impedance

The impedance of a junction diode is limited by dark current-contributing mechanisms operating in the given diode. In HgCdTe junctions, the known [10]–[13] contributing mechanisms are thermal diffusion of minority carriers, generation-recombination (GR) of carriers in the depletion region, trap- assisted-tunnelling, band-to-band tunnelling, and ohmic currents. The ohmic component owes its origin to surface leakage currents and/or dislocations intersecting the junction. Since the present work is essentially the extension of our previous paper [1], it will be sufficient here to consider diffusion, GR, and ohmic components due to dislocations. Consequently, the resultant zero-bias impedance of the diode will be calculated by using the following expression:

$$\frac{1}{R_0} = \frac{1}{R_{\text{diff0}}} + \frac{1}{R_{\text{gr0}}} + \frac{NA_j}{R_S}. \tag{15}$$

Here, A_j is the planar junction area, and $R_{\text{diff0}}, R_{\text{gr0}}$, and R_s are the impedances due to the diffusion current, GR current contribution, and individual dislocations, respectively.

The diffusion current impedance is given by

$$R_{\text{diff0}}^{-1} = \frac{q^2}{kT}\frac{n_i^2}{N_d}\frac{D_h}{L_h}A_j \times \frac{S_r\tau_h \cosh\left(\frac{t}{L_h}\right) + L_h \sinh\left(\frac{t}{L_h}\right)}{S_r\tau_h \sinh\left(\frac{t}{L_h}\right) + L_h \cosh\left(\frac{t}{L_h}\right)} \tag{16}$$

where S_r is the surface recombination velocity at the epi-substrate interface, t is the thickness, and N_d is the concentration of the donors in the base n-layer. In case of fully ionised donors, N_d will be equal to n_0.

The GR current impedance is given by

$$R_{\text{gr0}}^{-1} = \frac{q^2 n_i W_{\text{dep}} A_j}{2kT\tau_{\text{gr}}} \tag{17}$$

where W_{dep} is the depletion layer width, τ_{GR} is the GR lifetime of the minority carriers, and the impedance due to individual dislocations is given by

$$R_S^{-1} = \frac{2\pi q^2 n_i \text{smat}}{kT}. \tag{18}$$

III. Results and Discussions

Before we begin discussing the comparison of the results of model calculations with the experimental data, let us first have a look at some of the important predictions of the theoretical model, which will be required later to understand and explain the behavior of experimental data. Fig. 1 shows the shunt resistance contribution (R_s/N, in units of Ω-cm^2) due to dislocations in the base material as a function of the magnitude of space charge Q_{sc} (cm^{-2}) around the core of a dislocation and the location of the trap levels (E_t) contributing to the dislocation recombination. It is observed that the shunt resistance contribution due to dislocations is a very steep function of both Q_{sc} and E_t in a selected range of charges. In other words, small variations in Q_{sc} may lead to sharp variations in the shunt resistance. As will be seen later, the case under discussion belongs to this category, and many features of the experimental data of [2] can be now understood on this basis.

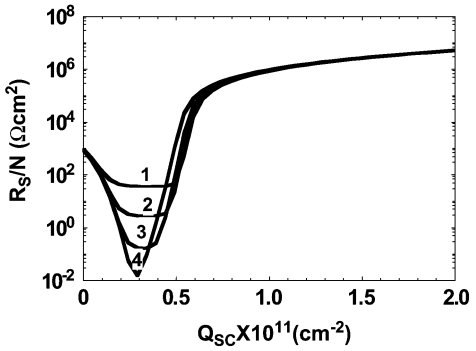

Fig. 1. Calculated dislocation shunt resistance at 40 K as a function of space charge density and the location of the trap level in an n-type $Hg_{1-x}Cd_xTe$ material having a dislocation density of 1×10^7 cm^{-2}. Curves labeled 1, 2, 3, and 4, respectively, correspond to trap level locations at 11, 20, 30, and 40 meV below the conduction band edge.

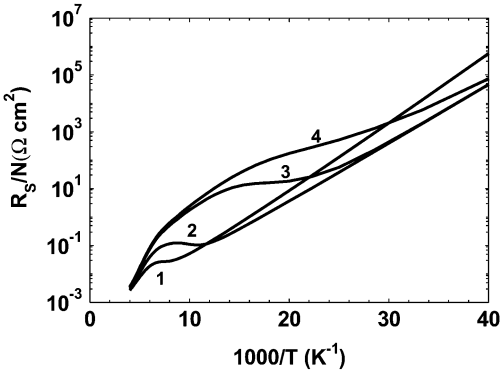

Fig. 2. Temperature dependence of the dislocation shunt resistance as a function of space charge density in an n-type $Hg_{1-x}Cd_xTe$ material having a dislocation density of 1×10^7 cm^{-2}. The location of the trap level is 11 meV below the conduction band edge. Curves labeled 1, 2, 3, and 4, respectively, correspond to space charge density of 1×10^{10} cm^{-2}, 3×10^{10} cm^{-2}, 5×10^{10} cm^{-2}, and 5.4×10^{10} cm^{-2}.

The temperature dependence of shunt resistance contribution as a function of Q_{sc} is shown in Fig. 2. It is seen that in the relatively high temperature (>150 K) region, the shunt resistance exhibits faster variation as compared to the intermediate temperature range. In conformance with a slowly varying shunt resistance contribution around 80 K, as seen from Fig. 2, some experimental studies have also reported [13]–[15] negligible shunt resistance variation in HgCdTe diodes in the same temperature range. Again, at temperatures of less than 50 K, shunt resistance is largely dependent on Q_{sc}. In summary, the temperature dependence of shunt resistance due to dislocations is a sensitive function of Q_{sc} and, thus, a temperature dependent study of shunt resistance or R_0 A could provide a fair estimate of charges around the core of dislocations.

The various parameters used in the above calculations are summarized in Table I and correspond to a material of 9.5-μm cutoff wavelength at 77 K. These parameters are practically the same as reported earlier [1] with the exception that the convention of indicating the location of trap level is now used as

TABLE I
MATERIAL PARAMETERS USED IN THE CALCULATIONS

Parameter	Symbol	Value	Reference
Electron concentration in n-region	N_d (fully ionised donors)	$1x10^{15}cm^{-3}$	1,19
Hole concentration in p^+-region	N_a	$1.7x10^{17}cm^{-3}$	1,19
Minority carrier mobility	μ_h	500 $cm^2 V^{-1}sec^{-1}$	1,19
77K cut-off wavelength	$\lambda_{cut-off}$	9.5μm (Array 1) 10.3 μm (Array 2)	2
Trap energy level	E_t	E_c-0.011eV	1,8
Capture cross-section for holes	K_p	$1x10^{-8}cm^3sec^{-1}$at 77K	1,8,20
Capture cross-section for electrons	K_n	$9x10^{-10}cm^3sec^{-1}$ at 77K	1,8,20
Surface state density	N_t	$1x10^{15}cm^{-2}$	1,9
space charge density	Q_{sc}/q	$5.4x10^{10}cm^{-2}$ (array1) $5.2x10^{10}cm^{-2}$ (array2)	1
Lattice constant of the base material.	a	$6.4x10^{-8}cm$	21
Energy Bandgap	E_g	in eV	Calculated using the expression given in Ref.22
Intrinsic carrier concentration	n_i	in cm^{-3}	Calculated using the expression given in Ref.23

$E_t = E_c - 0.011$ eV in place of $E_t = 1.4\ E_i$. This change became necessary [8] for the ease of indicating the location of trap levels from the conduction and valance band edges, respectively, in n- and p-type materials.

A. Temperature Dependence of R_0A Product

In this section, we will present the results of model calculations and compare them with the reported experimental data of Johnson *et al.* [2]. Some of the experimental details of the work of Johnson *et al.* are, however, first reproduced here for the sake of completeness. High-performance p-on-n double layer heterojunction LWIR detector arrays of mesa diodes were fabricated by growing HgCdTe epilayers on lattice-matched CdZnTe substrates by infinite melt technique in a vertical liquid phase epitaxy setup from a Hg-rich solution. Dislocations were induced by intentionally indenting the arrays close to the diodes with a modified tweezer tip. After the measurements of the diode characteristics, the dislocations within the diodes were revealed by using a defect etchant [16] and were found to lie on $\{111\}$ slip planes by X-ray Laue back-reflection measurements. The etch-pit-density for each diode was determined by dividing the number of etch pits in the diode area by the junction area A_j.

Fig. 3 shows the experimental results (squares) on the temperature dependence of an R_0A product of a high-performance p-on-n diode from an LWIR HgCdTe array fabricated in a high-quality HgCdTe epilayer. These results correspond to a diode with zero etch pit [2]. Experimental data shown by the circles is the measured performance of the diode with dislocation density of 1×10^7 cm^{-2} after indentation. Broken lines represent the previously reported [1] theoretical curves without taking into account the temperature dependence of minority carrier lifetime. Continuous line curves in Fig. 3 show theoretically predicted R_0A variation by the model after taking into account the temperature dependence of minority carrier lifetime. Numbers marked

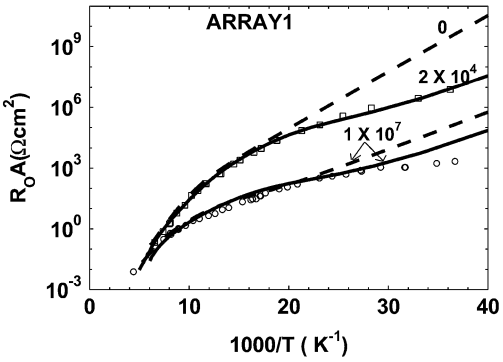

Fig. 3. Variation of R_0A with temperature for diodes of array1 with 9.5-μm cutoff wavelength and dislocation densities *N* marked on the curves. The points correspond to the experimental data of Johnson *et al.* [2], while the continuous and broken line curves, respectively, are the theoretically simulated curves using the present model with and without including the temperature variation of minority carrier lifetime.

on each of the calculated curves represent the dislocation density used in the calculation of the respective curve. In this figure, the continuous line curve for zero dislocations is not shown as it coincides with the corresponding broken line curve in the absence of dislocation contribution.

It can be observed from Fig. 3 that the theory (continuous line) agrees with the experiment over the entire temperature range, if we assume a dislocation density of 2×10^4 cm^{-2} in place of zero dislocation density. Growth of mercury cadmium telluride epilayers with dislocation density as low as 1×10^4 cm^{-2} have been reported in the published literature [17]. Additionally the number of dislocations per diode for a dislocation density of 2×10^4 cm^{-2} work out to be 0.14 for a diode junction area of 6.8×10^{-6} cm^2, practically consistent with the observations of zero etch pit by Johnson *et al.* [2]. Next, one can further observe vast improvement in the agreement between theory and experiment in case of diode of dislocation density 1×10^7 cm^{-2},

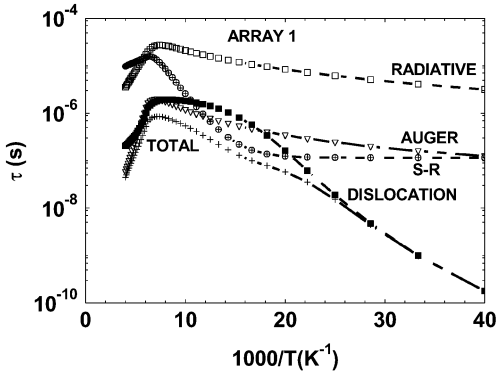

Fig. 4. Relative contributions due to radiative, Auger, SR and dislocation recombination mechanisms to minority carrier lifetime as a function of temperature in the base material (n-type MCT) in array1 for dislocation density of 1×10^7 cm^{-2}.

except some deviations below 33 K. The interaction of dislocations among themselves could be one possibility in the higher dislocation density range and will be discussed later.

It may be worthwhile to mention here that, 1) though the deviations between theory and experiment are generally qualitatively assigned to the tunnelling currents below 50 K, our calculations show (results not shown here) that the trap assisted and band-to-band tunnelling mechanisms contribute negligibly at zero bias, and 2) the temperature dependence of Auger and SR lifetime alone is not enough to take care of the disagreement between theory and experiment in the low ($<$50 K) temperature range. It is the contribution of dislocations, which dominate at low temperatures and account for the observed deviations. This point can be clearly seen from Fig. 4, which shows a comparison of the relative contributions due to radiative, Auger, SR and dislocation recombination mechanisms to the minority carrier lifetime in n-type HgCdTe. The present results are also in agreement with the statement of Shin *et al.* [18] that the high defect density limits the LWIR HgCdTe device performance at low temperatures $\sim$40 K.

In the end, it is concluded that the inclusion of the temperature dependence of minority carrier lifetime, in addition to the dislocation dependence, has resulted in the considerable improvement in the previously proposed model [1]. This is evident from the agreement of the experimental data and the theory over a broad range of temperature down to 25 K. Our past understanding in regard to the tunnelling currents as a possible source of disagreement between theory and experiment below 50 K may, therefore, be not correct.

B. Dislocation Dependence of R_0A Product

In the previous paper [1], we have discussed the dislocation dependence of R_0A product at 120 and 77 K. The 40 K data and its discussions were not then included primarily because the model deviated from the experiment at this temperature. With the current improvements in the model, it will be now appropriate to complete the discussions on 40 K data also. Discrete points indicated by circles in Figs. 5 and 6 show the experimentally reported [2] dislocation dependence of R_0A product of array 1 (78 K cutoff wavelength 9.5 μm) and array 2 (78 K cutoff wavelength 10.3 μm) at 40 K. The continuous line curve in each

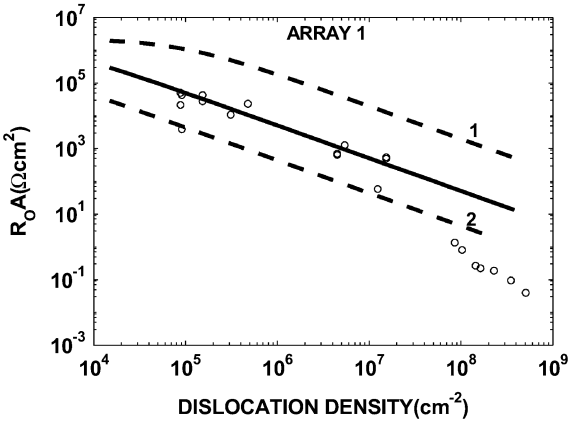

Fig. 5. Variation of R_0A with dislocation density at 40 K in diodes of array 1. Points are the experimental data taken from [2], while continuous and broken line curves are simulated theoretically using the present model. Continuous line curve corresponds to a space charge density ($Q_{\rm SC}$) of 5.4×10^{10} cm^{-2} and trap energy level at 11 meV below the conduction band edge. The broken line curves marked 1 and 2 correspond to $Q_{\rm sc}$ within $\pm 10\%$ of the value mentioned in Table I.

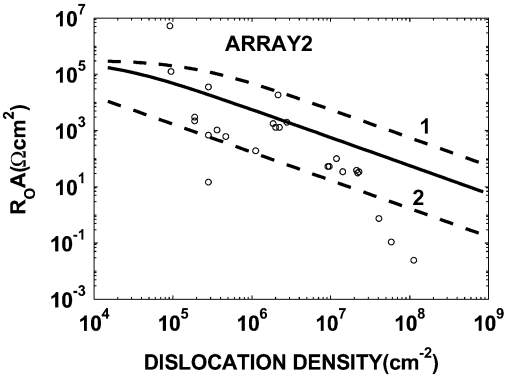

Fig. 6. Variation of R_0A with dislocation density in diodes of array 2. Points are the experimental data taken from the data of Johnson *et al.* [2], while continuous and broken line curves are simulated theoretically using the present model. Continuous line curve corresponds to a space charge density ($Q_{\rm SC}$) of 5.2×10^{10} cm^{-2} and trap energy level at 11 meV below the conduction band edge. The broken line curves marked 1 and 2 correspond to $Q_{\rm sc}$ within $\pm 10\%$ of the value mentioned in Table I.

figure represents the theoretically generated dislocation dependence using the parameters from Table I. The broken line curves marked 1 and 2 in each figure were theoretically generated by varying the charge $Q_{\rm sc}$ within $\pm 10\%$ of the value mentioned in Table I. It is observed that the general trend of the experimental data can be well accounted for by the present model (continuous line curve) for dislocation densities of less than 1×10^7 cm^{-2}. Further it is also seen that the scatter of the data up to dislocation density of 1×10^7 cm^{-2} is contained within the broken lines on either side of the continuous line indicating some kind of statistical variations in $Q_{\rm sc}$ within $\pm 10\%$ of the average value of the charge around the core of dislocations. However, at high dislocation densities of greater than 1×10^7 cm^{-2}, there are considerable deviations between theory and experiment. Similar observations were made in the previous paper [1] even at relatively higher temperatures, that is, 77 and 120 K. The clustering of dislocations at high dislocation densities was then considered as one of the possible options to explain the difference between theory and experiment. Alternatively, it is now suggested that

above dislocation density of 1×10^7 cm^{-2}, the theory can take care of observed deviations, by varying $Q_{\rm sc}$ in the descending order between $4.7 - 4.3 \times 10^{10}$ cm^{-2} and the location of trap level as $E_c - 0.02$ eV for array 1. Similarly, in the case of array 2, $Q_{\rm sc}$ shows a variation between $4.3 - 3.7 \times 10^{10}$ cm^{-2} with trap level at $E_c - 0.02$ eV. The systematic reduction in the value of the charge around the core of dislocations and the shift in the location of the trap level contributing to the carrier recombination appear to point out toward interaction of dislocations taking place above dislocation densities of 10^7 cm^{-2}. At higher densities, the dislocations are relatively closely spaced and may well interact with each other. Intuitively, the interaction among dislocations could be a function of dislocation density as well as the temperature of measurement. The reported deviations between theory and experiment below 33 K (see Fig. 3) may be assigned to the interaction of dislocations at dislocation densities of 1×10^7 cm^{-2}.

IV. Summary

This paper has emphasised the importance of taking in to account the temperature and dislocation dependence of minority carrier lifetime in the modeling of zero-bias resistance area product $(R_0{\rm A})$ of LWIR HgCdTe diodes. Dislocations are shown to play a dominant role in shaping the variation of R_0A product in the low temperature range. Physically, dislocations, besides acting as a shunt, influence the diode impedance through their effect on minority carrier lifetime. The shunt resistance contribution due to a dislocation has been found to be a very sensitive function of the charge around its core. Several features in the trend of the experimental data can be understood on the basis of variations in the charge around the core of dislocations either due to statistical variations or as a result of interaction of dislocations among themselves. The latter effect becomes visible at high dislocation densities of 1×10^7 cm^{-2} and above.

Acknowledgment

The authors would like to thank the Director, Solid State Physics Laboratory, Delhi, for his kind permission to publish this work.

References

[1] V. Gopal and S. Gupta, "Effect of dislocations on the zero-bias resistance-area product, quantum efficiency, and spectral response of LWIR HgCdTe photovoltaic detectors," *IEEE Trans. Electron. Devices*, vol. 50, pp. 1220–1226, May 2003.

[2] S. M. Johnson, D. R. Rhiger, J. P. Rosebeck, J. M. Peterson, S. M. Taylor, and M. E. Boyd, "Effect of dislocations on the electrical and optical properties of long-wavelength infrared HgCdTe photovoltaic detectors," *J. Vac. Sci. Technol. B, Microelectron. Process. Phenom.*, vol. 10, pp. 1499–1506, July/Aug. 1992.

[3] V. C. Lopes, A. J. Syllaios, and M. C. Chen, "Minority carrier lifetime in mercury cadmium telluride," *Semicond. Sci. Technol.*, vol. 8, pp. 824–841, 1993.

[4] J. S. Blakemore, *Semiconductor Statistics*. New York: Pergamon, 1962.

[5] P. E. Peterson, "Auger recombination in $Hg_{1-x}Cd_xTe$," *J. Appl. Phys.*, vol. 41, pp. 3465–3467, 1970.

[6] M. A. Kinch, M. J. Brau, and A. Simmons, "Recombination mechanisms in 8–14 μHgCdTe," *J. Appl. Phys.*, vol. 44, pp. 1649–1663, 1973.

[7] W. Shockley and W. T. Read, "Statistics of the recombination of holes and electrons," *Phys. Rev.*, vol. 87, pp. 835–842, 1952.

[8] V. Gopal and S. Gupta, "Effect of dislocations on minority carrier lifetime in HgCdTe," *J. Appl. Phys.*, vol. 95, pp. 2467–2472, 2004.

[9] A. Many, Y. Goldstein, and N. B. Grover, "Semiconductor Surfaces," , Amsterdam, The Netherlands: North-Holland, 1965, p. 197.

[10] M. B. Riene, A. K. Sood, and T. J. Tredwell, "Photovoltaic Infrared Detectors," , R. K. Willardson and A. C. Beer, Eds. New York: Academic, 1981, p. 201.

[11] A. Rogalski, "Photovoltaic detectors," in *Infrared Photon Detectors*, A. Rogalski, Ed. Bellingham, WA: SPIE, 1995, p. 56.

[12] V. Gopal, S. K. Singh, and R. M. Mehra, "Analysis of dark current contributions in mercury cadmium telluride junction diodes," *Inform. Phys. Technol.*, vol. 43, pp. 317–326, 2002.

[13] V. Gopal, S. Gupta, R. K. Bhan, R. Pal, P. K. Chaudhary, and V. Kumar, "Modeling of dark characteristics of mercury cadmium telluride n^+-p junctions," *Inform. Phys. Technol.*, vol. 44, pp. 143–152, 2003.

[14] R. S. List, "Electrical effects of dislocations and other crystallography defects in HgCdTe n-on-p photodiodes," *J. Electron. Mater.*, vol. 22, pp. 1017–1025, 1993.

[15] V. Gopal and S. Gupta, "Temperature dependence of ohmic shunt resistance in mercury cadmium telluride junction diode," *Inform. Phys. Technol.*, vol. 45, pp. 265–271, 2004.

[16] I. Hanhert and M. Schenk, "New defect etchants for CdTe and $Hg_{1-x}Cd_xTe$," *J. Cryst. Growth*, vol. 101, pp. 251–255, 1990.

[17] B. Pelliciari, "State-of-the-art of LPE HgCdTe at LIR," *J. Cryst. Growth*, vol. 86, pp. 146–160, 1988.

[18] S. H. Shin, J. M. Arias, D. D. Edwall, M. Zandian, J. G. Pasko, and R. E. DeWames, "Dislocation reduction in HgCdTe on GaAs and Si," *J. Vac. Sci. Technol. B, Microelectron. Process. Phenom.*, vol. 10, pp. 1492–1498, 1992.

[19] S. P. Tobin, M. H. Weiler, M. A. Hutchins, T. Parodos, and P. W. Norton, "Advances in composition control for 16 μM LPE P-on-n HgCdTe heterojunction photodiodes for remote sensing applications at 60 K," *J. Electron. Mater.*, vol. 28, pp. 596–602, 1999.

[20] J. Yoshino, J. Morimoto, H. Wada, A. Ajisawa, M. Kawano, and N. Oda, "Studies of relationship between deep levels and R_0A product in mesa type HgCdTe devices," *Opto.-Electron. Rev.*, vol. 7, pp. 361–367, 1999.

[21] P. Capper, "Properties of narrow gap cadmium-based compounds," , P. Capper, Ed. London, U.K.: Inspec, IEE, 1991, p. 41.

[22] G. L. Hansen, J. L. Schmit, and T. N. Casselman, "Energy gap versus alloy composition and temperature in $Hg_{1-X}Cd_XTe$," *J. Appl. Phys.*, vol. 53, pp. 7099–7101, 1982.

[23] G. L. Hansen and J. L. Schmit, "Calculation of intrinsic carrier concentration in $Hg_{1-X}Cd_XTe$," *J. Appl. Phys.*, vol. 54, pp. 1639–1640, 1983.

Vishnu Gopal received the M.Sc. degree in physics from Agra University, Agra, India, in 1965 and the Ph.D. degree, also in physics, from Meerut University, Meerut, India, in 1984.

His research interests include the optical and electrical characterization of semiconductor materials, ion implantation studies in semiconductors, IR detectors, and focal plane arrays. He is the author or coauthor of 107 research papers published in refereed international journals and presented/published in the Proceedings of national and international conferences. He joined Solid State Physics Laboratory, Delhi, India, in 1967 and is currently guiding the activity on the development of IR detectors in the laboratory as Associate Director.

Dr. Gopal is listed in Marquis' International *Who's Who in the World.*

Sudha Gupta received the M.Sc. degree in physics in 1986 from the University of Delhi, Delhi, India.

She joined Solid State Physics Laboratory, Delhi, in 1987 and is currently with the IR division working on the development of IR detectors and focal plane arrays.